Modeling Thermal and Optical Effects on Photopolymerization Systems

Allison K. O'Brien[†] and Christopher N. Bowman*[,†,‡]

Department of Chemical Engineering, University of Colorado, Boulder, Colorado 80309-0424, and Department of Restorative Dentistry, University of Colorado Health Sciences Center, Denver, Colorado 80045-0508

Received January 21, 2003; Revised Manuscript Received June 25, 2003

ABSTRACT: A comprehensive photopolymerization model that incorporates heat and mass transfer effects, diffusion-controlled propagation and termination, and temporal and spatial variation of species concentration, temperature, and light intensity is applied to systems with varying thermal and optical properties. The absorbance of the polymerizing system is varied by altering either the initiator concentration, sample thickness, or molar absorption coefficient of the initiator. Simulations show that the choice of initiator and sample thickness limits the initiator concentration usable to achieve complete conversion in a sample. Similarly, the initiator and its concentration should independently be chosen since each impact the polymerization differently. Three different thermal boundary conditions and their effects on polymerization are also considered. These boundary conditions include isothermal, perfectly insulating, and perfectly conducting. Simulations show that a higher absorbance sample polymerizes completely when perfectly insulating boundary conditions are assumed. Thus, it was found that the choice of initiator and its concentration should be determined not only from the desired film thickness but also considering the thermal conditions that affect the sample during photopolymerization.

1. Introduction

Photopolymerization of multivinyl monomers is a widely accepted and growing process. Countless products are produced utilizing photopolymerization including paints, coatings, adhesives, inks, microelectronics, optical materials, and dental resins.[1] The extensive uses and applications of photoinitiated polymerization are due to its many advantages over other polymerization processes, including that they are rapid, have reduced energy requirements, readily occur at room temperature, and are low cost.[1] The polymerizations are spatially and temporally controllable as the initiating light is resolvable in both space and time, respectively.[2] Additionally, the initiation rate is dictated by the choice of photoinitiator (i.e., its molar absorption coefficient, quantum yield, and efficiency), light intensity, and temperature. In photopolymerizations the monomer is often polymerized in bulk, eliminating the need for environmentally hazardous solvents. Finally, if multivinyl monomers are used, then cross-linking of the resulting polymer occurs, imparting unique physical properties to the product. Unfortunately, despite all of these benefits, there still exist many limitations, including oxygen inhibition and attenuated penetration of the light source into the sample.

The attenuation of the curing light by the sample often limits the ultimate polymer thickness and is caused by the absorption of light by the initiator, following the Beer−Lambert law. This phenomenon causes the polymerizing sample to become heterogeneous due to the different initiation rates and subsequent functional group conversions occurring throughout the depth of the sample. Light attenuation limits the cure depth in a sample to be polymerized in a nonphotobleaching system and greatly increases the necessary cure time for complete conversion in a photobleaching system. In polymerizing systems with photobleaching initiators, a frontal polymerization is often observed as the initiator is consumed, and the light penetrates more deeply into the sample. This frontal polymerization has been well documented and modeled by several researchers. Miller et al., Ivanov and Decker, and Terrones and Pearlstein have mathematically modeled simple polymerizing systems with photobleaching initiators.[3−6] Their models predict the heterogeneous initiator concentration distribution and the resulting initiation rate. Their results show the importance in choice of photoinitiator (molar absorption coefficient) and initiator concentration based on the desired sample thickness and application.

The models discussed above give accurate and useful predictions for optical effects on thick, isothermal systems. They simulate the basic trends observed due to absorbance and initiator concentration. However, some polymerization systems are more complex and necessitate the inclusion of additional factors such as heat generation and transfer, mass transfer, and diffusion-controlled kinetics. Under these conditions, the optimal initiator and its concentration may be different than those predicted by previous models. Thus, a broader, more comprehensive model needs to be applied to these photopolymerizable systems to investigate the effect of absorbance more completely.

Our work focuses on applying a comprehensive photopolymerization model, based on that of Goodner and Bowman, to photobleaching photopolymerizing systems under a variety of absorbance and heat transfer conditions.[7−9] The model incorporates heat and mass transfer effects as well as species, temperature, and light intensity variation through the sample depth while also utilizing a realistic model of the diffusion-controlled polymerization kinetics. The objective of this work was to investigate the effects of absorbance and thermal boundary conditions on the resulting photopolymerization kinetics. The absorbance, A, is defined as the product of the initiator concentration, molar absorption coefficient of the initiator, and depth of the sample. The absorbance was adjusted by varying either the molar absorption coefficient, the thickness of the sample, or the initiator concentration. Three different thermal

[†] University of Colorado.
[‡] University of Colorado Health Sciences Center.
* To whom correspondence should be addressed: Fax 303-492-4341; e-mail bowmanc@colorado.edu.

10.1021/ma034070c CCC: $25.00
Published on Web 08/23/2003

conditions were explored, including two conducting surfaces, two insulated surfaces, and isothermal samples.

2. Model Description

The simulation developed for this work is a comprehensive kinetic model describing photopolymerization that allows for variation of temperature, species concentration, and light intensity throughout the thickness of the polymerizing film. The model is based on the classical mechanisms for free radical polymerization. This includes initiation, propagation, and termination, whereby, in this case, initiation occurs from the photolysis of the initiator. Heat and mass transfer effects as well as diffusion-controlled propagation and termination are incorporated. Heat effects are important as the kinetic constants as well as the diffusion coefficients are functions of temperature. Diffusion of small species is an important aspect of photopolymerizations, and thus, mass transfer is also critical. The complete model development was described in previous work,[7−9] while the additional ability to simulate both photobleaching and nonphotobleaching photoinitiators was incorporated into this current work.

2.1. Energy Balance. Energy transport has been incorporated into the 1-D simulation through an energy balance that includes heat accumulation, heat transfer, and heat generation by reaction and radiation absorption as shown in eq 1. Heat generation by reaction is due to the exothermic nature of the polymerization reaction. The absorbing species is primarily the initiator molecules as most monomers and polymers are transparent in the ultraviolet region. The resulting energy balance is determined:

$$\rho C_p \frac{\mathrm{d}T}{\mathrm{d}t} = k \frac{\mathrm{d}^2T}{\mathrm{d}z^2} - \Delta H \frac{\mathrm{d[C{=}C]}}{\mathrm{d}t} + \epsilon I_{\mathrm{inc}} c_{\mathrm{I}}^* \qquad (1)$$

In this equation, ρ and C_p are the density and heat capacity, k is the thermal conductivity, z is the spatial coordinate for sample depth, ΔH is the heat of polymerization, the derivative d[C═C]/dt represents the consumption of double bonds through polymerization, ϵ is the molar absorption coefficient of the initiator, I_{inc} is the incident light intensity, and c_{I}^* is the concentration of all absorbing initiator moieties in the slice. The variable c_{I}^* accounts for unreacted initiator molecules in photobleaching systems. The last term in the energy balance assumes that all absorbed energy is converted to heat.

The thermal boundary conditions at the top and bottom of the sample may be either perfectly conducting or perfectly insulating. Additionally, the entire sample can be held isothermal. A sample with two constant temperature surfaces (perfectly conducting) simulates a sample laminated with a highly thermally conductive substrate, such as metal, or in contact with air when there is sufficient heat removal by convection. A sample with two insulating surfaces (adiabatic system) imitates a system laminated between low thermal conductivity substrates.

2.2. Species Balance. In the 1-D simulation, mass transfer has been incorporated through the addition of a diffusive flux term to the species balance. The general species balance is determined from the following:

$$\frac{\mathrm{d}c_i}{\mathrm{d}t} = \frac{\mathrm{d}}{\mathrm{d}z}\left(\hat{c} D_i \frac{\mathrm{d}\hat{x}_i}{\mathrm{d}z}\right) + R_i \qquad (2)$$

where the subscript i refers to the component. The first term is the species accumulation, the second term is the diffusive flux, and the third term is the consumption or generation by reaction. c_i is the concentration of species i, D_i is the diffusion coefficient of species i, and R_i is the reaction term for species i. The two variables $\hat{c}$ and $\hat{x}_i$ are the concentration of mobile species and mole fraction of mobile species, respectively. The mobile species are the initiator, monomer, and primary radicals. The classical photopolymerization mechanisms of initiation, propagation, and termination are incorporated into the reaction term. The species balances are conducted for initiator, primary radical, monomer, polymer radical, and dead polymer.

2.3. Further Model Information. Light attenuation throughout the sample is modeled using the Beer−Lambert law, which, for a photobleaching species, can be solved to obtain the light intensity profile as follows:

$$I = I_0 \mathrm{e}^{-\epsilon_1 c_{\mathrm{I}} z} \qquad (3)$$

In this equation, I is the light intensity at a depth z into the sample, I_0 is the incident light intensity at the top surface, ϵ_1 is the molar absorption coefficient of the initiator, and c_{I} is the unreacted initiator concentration.

The kinetic constants used in this work incorporate Arrhenius temperature dependence, diffusion-controlled kinetics, and termination by reaction diffusion. The latter two phenomena are described in terms of fractional free volume of the polymerizing mixture.

Several assumptions are incorporated into the model: (i) The light source is monochromatic at 365 nm, and the initiation reaction is assumed to generate two primary radicals of equal reactivity and mobility. (ii) To simulate the polymerization in a thick sample, the sample is divided into uniform slices over which the light intensity, species concentration, and temperature are constant within the slice. (iii) The volume of each of these slices is assumed to be constant over the course of the reaction. (iv) Propagation, termination, and inhibition are assumed to be chain length independent. (v) Bimolecular termination is characterized by a lumped k_{t} that accounts for both combination and disproportionation. (vi) Physical and thermal properties of the system (density, specific heat, and conductivity) are assumed to remain constant throughout the course of the reaction.

The model monomer used in the simulations is 2-hydroxyethyl methacrylate (HEMA) because it is monovinyl and exhibits chain length independent propagation and termination kinetics. The initiator used in the simulations is 2,2-dimethoxy-2-phenylacetephenone (DMPA), a common photoinitiator. The kinetic and physical parameters used have been previously described.[7]

3. Results and Discussion

Simulations were conducted to investigate the effects of absorbance and thermal boundary conditions on the resulting photopolymerization kinetics. The goal of the simulations was to explore the conditions and variables that directly affect light attenuation and polymerization kinetics in photopolymerizing samples. To vary the absorbance, A, either the molar absorption coefficient, the sample thickness, or the initiator concentration was adjusted. Three thermal boundary conditions were also considered including isothermal, perfectly conducting, and perfectly insulating. The effect of absorbance was

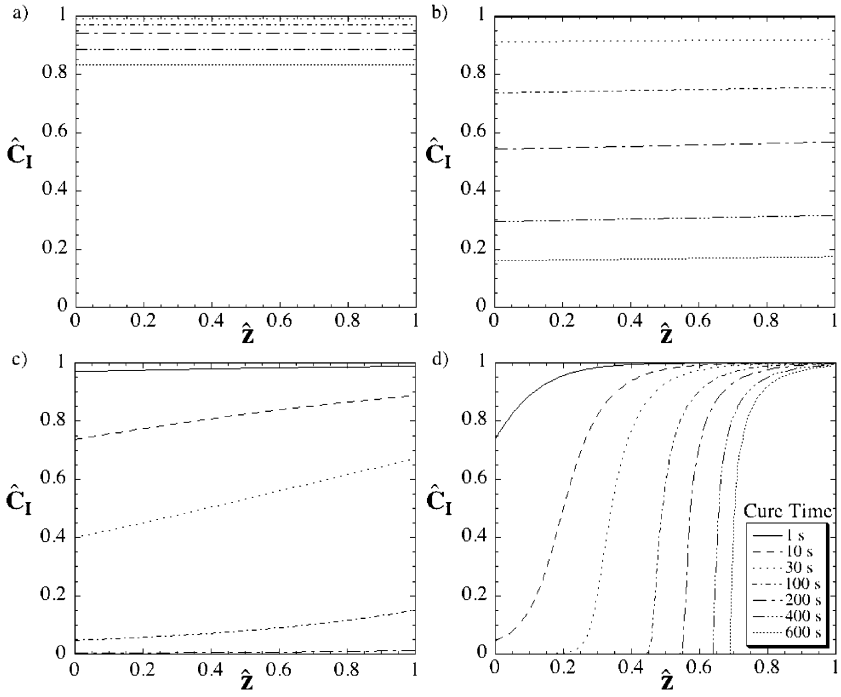

Figure 1. For an isothermal system, the effect of the molar absorption coefficient on the dimensionless photoinitiator concentration profiles, $\hat{C}_I$, as a function of dimensionless depth, $\hat{z}$. $\hat{C}_I = C_I/C_{I,0}$, the ratio of initiator concentration to the initial initiator concentration, where $C_{I,0} = 0.1$ M. $\hat{z} = x/L$, the ratio of the depth to the sample thickness, where $L = 0.01$ cm. (a) $\gamma = 0.01$, (b) $\gamma = 0.1$, (c) $\gamma = 1$, (d) $\gamma = 10$.

also considered for an isothermal system to isolate thermal effects. Similarly, the effect of thermal boundary conditions was investigated for varying optical densities by adjusting the initiator molar absorption coefficient.

3.1. Effect of Absorbance. The absorbance of the polymerizing sample dictates the degree of light attenuation. However, there are multiple variables that can be modified to change the absorbance, i.e. molar absorption coefficient of the initiator, initiator concentration, and sample thickness. At the same absorbance, it is possible to have many combinations of these three properties. Since the absorbance is the same, the samples will show the same initial light attenuation, but soon after, differences will be apparent as each variable has distinct influences on other aspects of the polymerization.

3.1.1. Molar Absorption Coefficient. Figure 1 illustrates the effect of the initiator molar absorption coefficient on the dimensionless photoinitiator concentration as a function of depth in an isothermal, photobleaching sample. The molar absorption coefficient of the initiator not only dictates the degree of light attenuation but also directly affects the initiation rate. The rate of initiation is defined as[2]

$$R_i = \phi\epsilon C_I(z,t)\, I(z,t) \tag{4}$$

Thus, as the initiator molar absorption coefficient, ϵ, is increased, not only will the light attenuation increase but also the initiation rate at the top surface will increase.

Figure 1a demonstrates that in a sample with very low absorbance there is minimal light attenuation (only 1% initially), and thus the initiator concentration is constant throughout the depth of the sample and decreases uniformly with time. As A or ϵ is increased in Figure 1a−d, the effect of light attenuation, initiation rate, and diffusion become more apparent. The characteristic diffusion time for these samples is $t_{diff} = L^2/D_I = (0.01\text{ cm})^2/2.2 \times 10^{-6}\text{ cm}^2/\text{s} = 45.5$ s. Thus, diffusion is not very important in these samples; however, it becomes apparent in the samples with large heterogeneity and slow polymerization. As ϵ is increased in Figure 1a−c, initiator is consumed more quickly due to the increase in photolysis rate. However, as ϵ is increased, light attenuation also increases, and a nonuniform consumption profile emerges and becomes apparent in Figure 1c,d. Figure 1d shows rapid photobleaching, where at 600 s, the initiator has essentially been consumed in over 70% of the sample. This result is due to the large increase in photolysis rate as shown in eq 4, which greatly overcomes the effect of increased light attenuation.

3.1.2. Sample Thickness. Figure 2 illustrates the effect of sample thickness on the dimensionless photoinitiator concentration at the same four optical densities studied in Figure 1. Although the optical densities are similar, significantly different results are found. Figure 1a shows very little photoinitiator consumption compared to Figure 2a, although they both have $A = 0.01$. The reason for this result is that the large difference in the molar absorption coefficient in the two samples results in dramatically different photolysis rates. In Figure 2a, the initiator is initially photolyzed 100 times faster than Figure 1a. This same trend is seen in comparing Figures 2b and 1b. In Figure 2c,d, nonuniform profiles arise due to the increase in light attenuation, similar to Figure 1c,d. However, in Figure 2d, initiator has been consumed in only 40% of the sample at 600 s as opposed to 70% in Figure 1d. This difference is due to the photolysis rate and thus the rate of photobleaching that occurs within each film. The rate is higher in Figure 1d due to the higher molar absorption coefficient. It can be seen, though, that the shapes of the profiles in Figures 1d and 2d are almost identical.

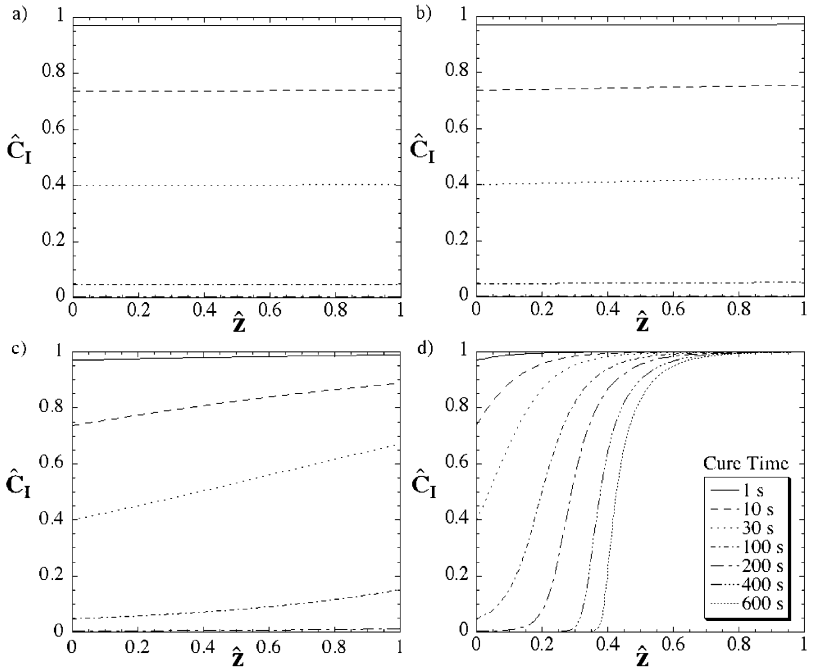

Figure 2. For an isothermal system, the effect of sample depth on dimensionless photoinitiator concentration profiles, $\hat{C}_I$, as a function of dimensionless depth, $\hat{z}$, where $\epsilon = 1000$ L/(mol cm). $\hat{C}_I = C_I/C_{I,0}$, the ratio of initiator concentration to the initial initiator concentration, where $C_{I,0} = 0.1$ M. $\hat{z} = x/L$, the ratio of the depth to the sample thickness. (a) $\gamma = 0.01$, (b) $\gamma = 0.1$, (c) $\gamma = 1$, (d) $\gamma = 10$.

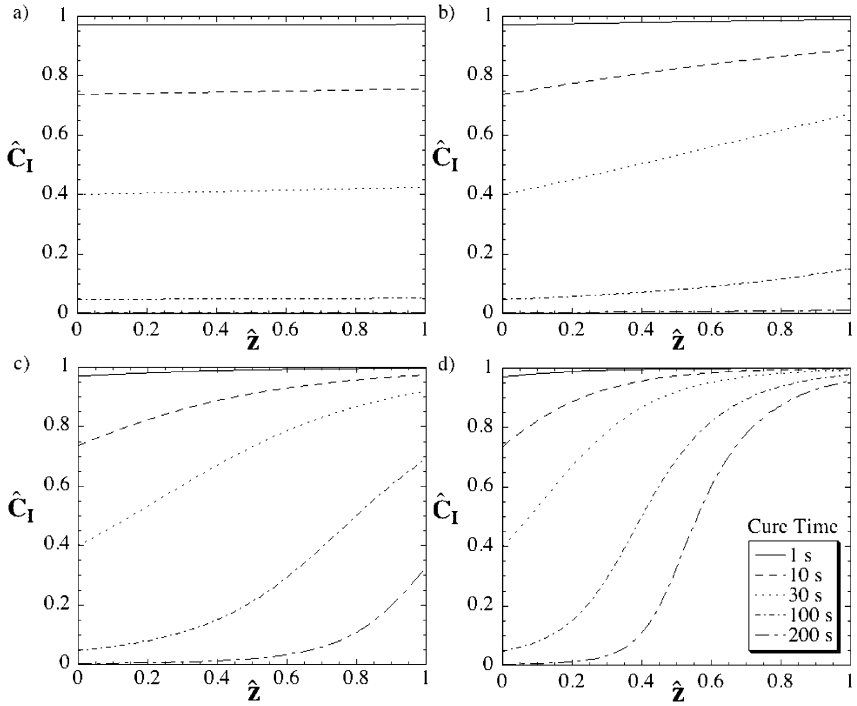

Figure 3. For an isothermal system, the effect of initiator photoinitiator concentration on dimensionless photoinitiator concentration profiles, $\hat{C}_I$, as a function of dimensionless depth, $\hat{z}$, where $\epsilon = 1000$ L/(mol cm). $\hat{C}_I = C_I/C_{I,0}$, the ratio of initiator concentration to the initial initiator concentration, and $\hat{z} = x/L$, the ratio of the depth to the sample thickness, where $L = 0.01$ cm. (a) $\gamma = 0.1$, (b) $\gamma = 1$, (c) $\gamma = 2.5$, (d) $\gamma = 5$.

3.1.3. Initiator Concentration. Figure 3 demonstrates the effect of initiator concentration on the dimensionless photoinitiator concentration profile. The initiator concentration plays two roles: as the absorbing species that attenuates the curing light and as a direct variable in controlling its photolysis rate. Thus, because of this synergistic effect, we would expect to see a more slowly moving front as the initiator concentration is increased since the photolysis rate will rapidly decrease as initiator is consumed. Figure 3 shows that, with a 50-fold increase in initiator concentration and absorbance, the system goes from one with uniform initiator consumption to that with a frontal polymerization that moves very slowly due to the decease in initiation rate and mobility.

In Figures 3a and 2b, identical profiles are found when they have the same absorbance value ($A = 0.1$) and molar absorption coefficient but different sample

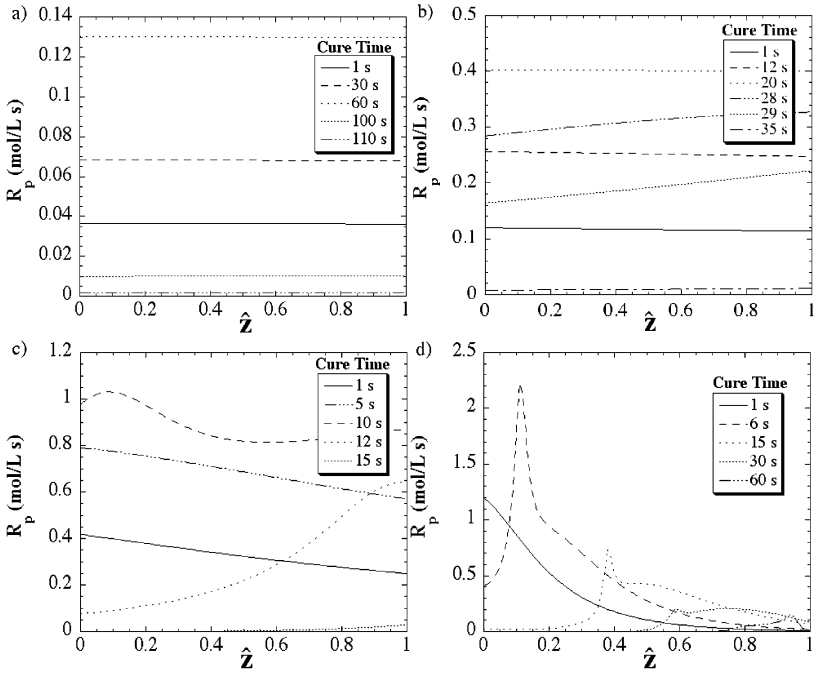

Figure 4. For a perfectly insulated system, the effect of the molar absorption coefficient on the polymerization rate as a function of dimensionless depth, $\hat{z}$, where $\hat{z} = x/L$, the ratio of the depth to the sample thickness, and $L = 0.01$ cm. $C_{I,0} = 0.1$ M. (a) $\gamma = 0.01$, (b) $\gamma = 1$, (c) $\gamma = 1$, (d) $\gamma = 10$.

thickness and initial initiator concentration. An additional simulation was run (not shown), where $A = 5$ ($\epsilon = 1000$ L/(mol cm), $L = 0.05$ cm, and $C_{I,0} = 0.1$ M), and compared to Figure 3d. Similarly, identical profiles were produced. These results show that if the molar absorption coefficients are the same, the sample thickness and initiator concentration do not affect the photobleaching rate, as long as the total absorption is the same. Additionally, when comparing Figures 1b and 3a, where $A = 0.1$, it is seen that the sample with the higher molar absorption coefficient (Figure 3a) photobleaches faster. Thus, it is clearly important to know all of the specific sample properties that determine overall light absorption, such as molar absorption coefficient, initiator concentration, and sample thickness.

3.2. Effect of Thermal Boundary Conditions. Heat transfer in a polymerizing sample is affected by the thermal boundary conditions. Heat is produced in the sample due to the heat of reaction and absorbed incident radiation. Insulating boundary conditions cause all of the energy to be retained as heat and thus greatly affect the temperature of the sample and the resulting kinetics and mobility. Conversely, constant temperature boundary conditions remove much of the heat produced. The resulting changes in the kinetics and mobility alter the effect that the absorbance would normally produce.

Figure 4 illustrates the effect of absorbance in an insulated system on the polymerization rate. Comparing parts a and c of Figure 4, it can be seen in part c that the light attenuation is 100 times greater, as are the initiation rate and temperature increase, and the polymerization rate is more than 100 times greater. This drastic increase in polymerization rate is due to increased kinetic parameters and mobility from the increase in sample temperature from absorbed incident radiation and more rapid evolution of heat by the reaction. In Figure 4c,d, the frontal polymerization becomes more apparent when the absorbance and the absorbed incident radiation are greater. The simulation shows heterogeneity within the depth of the sample, where initially the polymerization rate is higher at the top of the sample, and as the polymerization proceeds through the depth of the sample so does the polymerization rate maxima. The decrease in polymerization rate with increased sample depth is due to a decrease in polymer radical concentration, resulting from an increase in termination. This enhanced termination rate is a direct result of the temperature and mobility increase.

If we compare Figure 4 to the conducting system shown in Figure 5, much different profiles are found. As the absorbance is increased in Figure 5, the frontal polymerization becomes more apparent at a lower absorbance due to the decrease in mobility. In Figure 5d, the polymerization proceeds significantly only in the top 40% of the sample. However, in Figure 4d, the polymerization not only proceeds into the whole sample but also does so at a very rapid rate. The reason for this increased penetration is shown in Figure 6. As expected, a much larger temperature rise occurs in the insulated system, Figure 6a, compared to the conducting system in Figure 6b. This elevated temperature not only greatly increases all rate parameters but also keeps the sample above the T_g of the polymer (328 K), thus maintaining higher mobility in the polymer. The overall reaction then continues to completion due to the increased mobility. As a result of the insulating boundary conditions, complete reaction is achieved throughout the sample though it has a very large absorbance. This polymerization would not be possible in an isothermal system or one with two constant temperature surfaces.

4. Conclusions

In this work, the effects of absorbance and thermal boundary conditions on photopolymerizing systems have been studied utilizing a comprehensive kinetic model. The model incorporated diffusion-controlled propagation and termination as well as heat and mass transfer

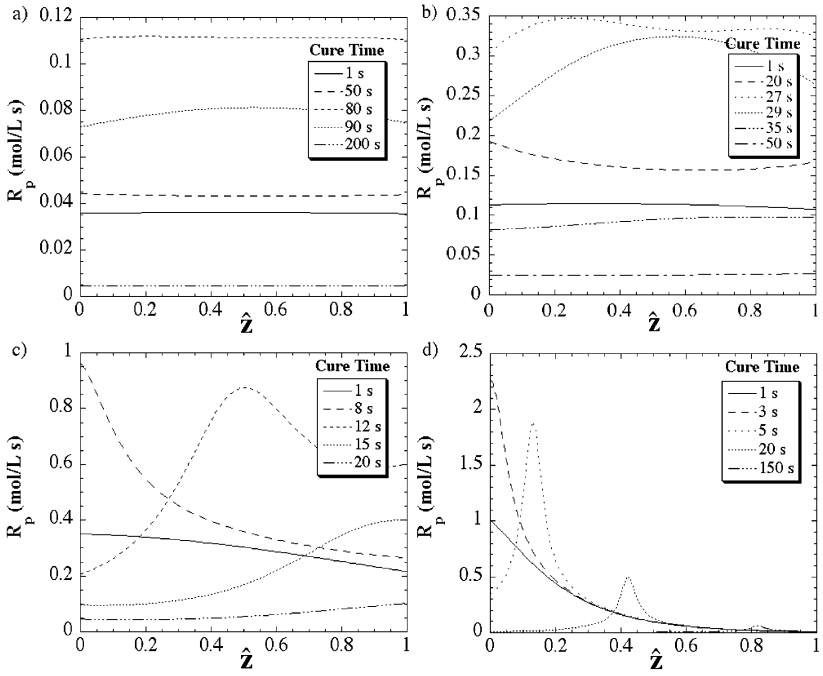

Figure 5. For a perfectly conducting system, the effect of the molar absorption coefficient on the polymerization rate as a function of dimensionless depth $\hat{z}$, where $\hat{z} = x/L$, the ratio of the depth to the sample thickness, and $L = 0.01$ cm. $C_{I,0} = 0.1$ M. (a) $\gamma = 0.01$, (b) $\gamma = 1$, (c) $\gamma = 1$, (d) $\gamma = 10$.

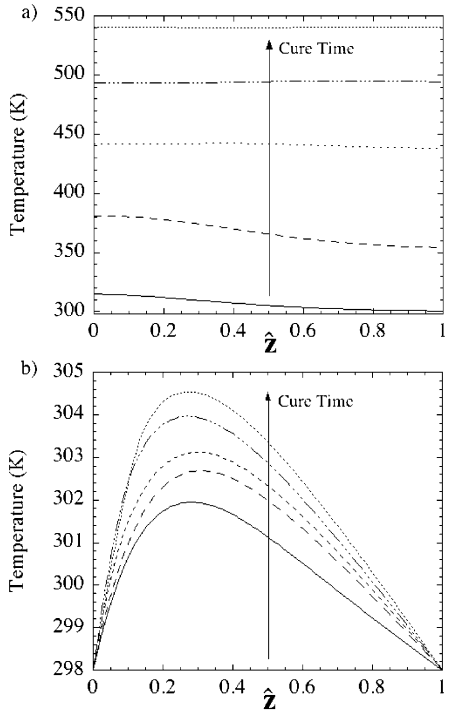

Figure 6. Temperature profiles in perfectly insulated (a) and constant surface temperature (b) samples where $\hat{z} = x/L$, the ratio of the depth over sample thickness. $\gamma = 10$, where $L = 0.01$ cm, $C_{I,0} = 0.1$ M, and $\epsilon = 10^4$ L/(mol cm). Times range from 1 to 30 s (a) and 1 to 10 s (b).

effects. The spatial and temporal development of the dimensionless initiator and polymerization rate profiles were presented and analyzed. Simulations demonstrated the effects of increasing absorbance and the differences that arise when adjusting distinct variables that affect absorbance. Simulations also illustrated the effect of thermal boundary conditions on systems with varying absorbance.

Model results illustrate that the choice of initiator and sample thickness limits the initiator concentration allowable to achieve complete conversion in a sample. Similarly, the initiator and its concentration should independently be chosen since each impacts the polymerization differently. Simulations show that a higher absorbance sample fully polymerizes with perfectly insulating boundary conditions due to the increase in mobility and kinetic parameters. Thus, on the basis of these simulations, the choice of initiator and initiator concentration should be determined not only from the desired film thickness but also from the thermal conditions on the sample during photopolymerization.

Acknowledgment. The authors thank the NSF I/UCRC for the Fundamentals and Applications of Photopolymerizations, the National Institute of Health (NIH Grant DE 10959) for research funding, and the Department of Education for granting a GAANN fellowship to A.K.O.

References and Notes

(1) Fouassier, J.-P. *Photoinitiation, Photopolymerization, and Photocuring*; Hanser/Gardner Publications: Cincinnati, OH, 1995.
(2) Odian, G. *Principles of Polymerization*; John Wiley & Sons: New York, 1991.
(3) Miller, G. A.; Gou, L.; Narayanan, V.; Scranton, A. B. *J. Polym. Sci., Part A: Polym. Chem.* **2002**, *40*, 793−808.
(4) Ivanov, V. V.; Decker, C. *Polym. Int.* **2001**, *50*, 113−118.
(5) Terrones, G.; Pearlstein, A. J. *Macromolecules* **2001**, *34*, 8894−8906.
(6) Terrones, G.; Pearlstein, A. J. *Macromolecules* **2001**, *34*, 3195−3204.
(7) Goodner, M. D.; Bowman, C. N. *Chem. Eng. Sci.* **2002**, *57*, 887−900.
(8) Goodner, M. D.; Bowman, C. N. *Macromolecules* **1999**, *32*, 6552−6559.
(9) Goodner, M. D.; Lee, H. R.; Bowman, C. N. *Ind. Eng. Chem. Res.* **1997**, *36*, 1247−1252.

MA034070C